The Ionospheric Conductances and the Characteristics of the Precipitating Electrons in the Auroral Region

Byung-Ho Ahn and Young-Sil Kwak

Department of Earth Science, Kyungpook National University, Taegu, Korea

(Manuscript received 2 November 1994)

Abstract

An attempt is made to establish empirical relationships between the ionospheric conductances measured from the Chatanika incoherent scatter radar and the magnetic disturbance data obtained simultaneously from the nearby College magnetic station. For this purpose the entire auroral region is divided into 30 sectors in terms of magnetic local time and the relative position with respect to the center of auroarl electrojet. The vertical component of magnetic disturbance is used in dividing the auroral electrojet into the poleward and equatorward halves. The empirical formulas thus obtained can be used in constructing the global conductance distribution on an instantaneous basis with the corresponding instantaneous magnetic disturbance data as input. The energy spectrum of precipitating electrons is further inferred on a global scale from the formulas incorporated with the ones proposed by *Robinson et al.* [1987].

Several interesting features noted in this study are : (1) The Hall conductance in the westward electrojet region is significantly higher than that in the eastward electrojet region for a given level of magnetic activity. Within the westward electrojet region the Hall conductance in the equatorward half is much higher than that in the poleward half. (2) The average energy of electrons does not seem to be very sensitive to magnetic activity. And the energy spectrum does not show any significant spatial variation with respect to the center of auroral electrojets. However, it changes significantly in the longitudinal direction with the minimum and maximum values being registered in the postnoon and morning sectors, respectively. (3) The energy flux of precipitating electrons show very similar spatial charateristics with those of Hall conductance, thus suggesting that the conductance enhancement is more closely associated with the flux increase than with the hardening of the energy spectrum. The most prominent energy flux during disturbed period is registered in the equatorward half of the westward electrojet between 20 MLT and 09 MLT. (4) Finally the particle characteristics inferred from the present study are quite comparable with the statistical study based on satellite particle measurements by *Hardy et al.* [1985] in terms of both magnitude and spatial distribution pattern.

1. INTRODUCTION

The knowledge of the global distribution pattern of electron precipitation over the polar ionosphere is crucial in the studies of magnetospheric electrodynamics and the magnetosphere-thermosphere ionosphere coupling. In particular, such an information is indispensable in determining the ionospheric conductivity distribution. So far particle measurements from low-altitude satellite have been utilized to estimate such an important parameter. Since particle detectors on board satellite can only provide information along its trajectory, however, it cannot provide an instantaneous two-dimensional information over the entire polar region. Therefore, it would be safe to say that the global electron precipitation pattern based on such satellite particle measurements can reflect at most a 'climatological' picture of the polar ionosphere. In spite of such a limitation the method has been widely adopted in estimating global electron precipitation pattern [*Hardy et al.*, 1985] and ionospheric conductivity distribution over the entire polar ionosphere [*Wallis and Budzinski*, 1981; *Spiro et al.*, 1982; *Fuller-Rowell and Evans*, 1987; *Hardy et al.*, 1987]

Recently magnetometer inversion methods [e.g., *Kamide et al.*, 1981; *Richmond and Kamide*, 1988] play an important role in probing the polar ionosphere and in studying magnetospheric electrodynamics. In particular, they have been improved to the point to provide high-time resolution (say, 5 min.) pictures of the electrodynamic quantities over the entire polar ionosphere. However, it is unfortunate to point out the fact that the methods adopt one of statistical conductance models based on satellite particle measurements. Thus the output from the magnetogram inversion method to be realistically instantaneous ones, a global instantaneous pattern of particle precipitation/ionospheric conductance distribution is indispensable.

By comparing the location of the auroral electrojet which was inferred from the meridian chain of magnetometer data and the luminous band of auroral emission determined by the auroral scanning photometer on board the ISIS 2 polar-orbiting spacecraft, *Wallis et al.* [1976] showed that the auroral electrojet is contained within the latitudinal range of auroral precipitation. The study indicates strongly the possibility that the conductivity enhancement is primarily responsible for the intensification of the auroral electrojet. *Ahn et al.* [1983] also noted that the intensification of the horizontal component (ΔH) of magnetic perturbation recorded at College was closely associated with the conductivity enhancement over the same region estimated from the nearby Chatanika incoherent scatter radar. Examining the close association between ΔH and simultaneously obtained ionospheric conductance, they were able to derive empirical relationships between the two quantities.

Recently *Rostoker et al.* [1985] reported that the energy spectrum of precipitating particles in the auroral region changes latitudinally. *Foster*[1987] showed further that the relative importances of electric field and ionospheric conductivity does vary spatially even within an auroral electrojet. More recently *Kamide* [1988] argued that there is a boundary which divides conductance-dominant and electric field-dominant westward electrojets.

Therefore, it is highly desirable to accommodate such recent findings into the model proposed by *Ahn et al.* [1983]. First to accommodate the Foster's finding, the vertical component of magnetic disturbance (ΔZ) can be utilized, since the sign of it provides the information about the relative position of the College magnetic observatory with respect to the center of the auroral electrojet. With such a convention it is possible to divide an auroral electrojet latitudinally into two halves, i.e., the poleward and equatorward halves in terms of the signs of the two components of magnetic disturbances. For example, the poleward

half of the westward electrojet carries the sign convention of $\Delta H < 0$ and $\Delta Z > 0$. Second the auroral electrojet are further subdivided longitudinally in terms of magnetic local time (MLT). Thus the entire auroral electrojet region can be divided by a number of sectors in terms of the signs of magnetic disturbances (ΔH, ΔZ) and magnetic local time.

2. Data Processing

The ionospheric conductance data used in the this study were obtained through the azimuthal scan mode in which the Chatanika antenna was held at constant elevation - usually somewhere between 60° and 80° - while it rotated 360° in azimuth within about 16 minutes. The three points measurements during each scan were made along the directions of, for example, 89°, 209° (magnetic south of the Chatanika radar) and 329° from the true north with about five minutes of integration times for each direction. With an elevation angle of 70°, the E region examined is about 40 km away from the radar site. When the electron density distribution within the altitude range of 90 km and 200 km is taken into account in estimating height-integrated conductivity (conductance), the diameter of the field view of the radar, corresponding to the spatial resolution of the conductance data, becomes about 140 km with an elevation angle of 70°during an azimuthal scan mode operation. The temporal resolution of the data is about 16 minutes, corresponding to the azimuthal scan period of the radar.

We are interested in only the conductance distribution due to auroral particle precipitation. However, the data obtained from the Chatanika radar are the combined results from both the solar EUV radiation and auroral particles. Thus we need to remove the solar component by employing one of widely used empirical formulas [for example, *Robinson and Vondrak*, 1984] usually expressed in terms of the solar zenith angle and Sa value, the daily value of the 10.7-cm solar radio flux. In this study we employ the formula proposed by *Kroehl and Richmond* [unpublished, 1988].

The ground magnetic disturbance data to be compared with the conductance data were simultaneously obtained from College, the closest standard magnetic station to the Chatanika incoherent scatter radar. Before comparing these two quantities the baseline value associated with the quiet time daily magneic variation is removed from the magnetic disturbance data. For the purpose a magnetic quiet day is selected for each month and the average value of the day is subtracted from the data obtained during the month. The data thus processed are further averaged over the azimuthal scan period of the radar.

The entire auroral electrojet system is divided into four regions based on the signs of ΔH and ΔZ components; that is, the polarward and equatorward halves of the eastward electrojet ($\Delta H>0$, $\Delta Z<0$; $\Delta H>0$, $\Delta Z>0$) and the same divisions for the westward electrojet ($\Delta H<0$, $\Delta Z>0$; $\Delta H<0$, $\Delta Z<0$). To investigate the magnetic local time dependence of precipitating particles, the four regions are further divided into 10 magnetic local time sectors; 12-19, 19-22 and 22-24 MLT sectors in the eastward electrojet region and 20-22, 22-24, 00-02, 02-04, 04-06, 06-09, and 09-12 MLT sectors in the westward electrojet region, thus the entire auroral region being divided into 20 zones. Since the two kinds of electrojets are frequently colocated over the local time sector between 20 MLT and 24 MLT, the region is examined twice by considering it either as the westward or eastward electrojet region.

By assuming that the energy spectrum of auroral particles is mostly Maxwellian in shape, *Robinson et al.* [1987] proposed the following expressions relating Hall and Pedersen conductances to the average energy (E) and energy flux (ϕ) of precipitating electrons

$$\Sigma_P = \frac{40\,E}{16+E^2}\,\phi_E^{1/2} \qquad (1)$$

$$\frac{\Sigma_H}{\Sigma_P} = 0.45(E)^{0.85} \qquad (2)$$

where Σ_P and Σ_H are the Pedersen and Hall conductances in mhos, respectively, E is the average energy in keV and ϕ_E is the energy flux in ergs/cm^2 · sec. Such empirical relationships can be used in inferring the average energy and energy flux of the precipitating electrons.

3. Results

(1) Ionospheric conductance

Figure 1 shows examples of the relationships between Hall conductance and ΔH in the eastward electrojet region ($\Delta H > 0$). Each data point in the figure represents a conductance measurement with a 16-min integration time. The upper and lower panels of the figure represent the relationships in the poleward and equatorward halves of the eastward electrojet region, respectively. To show the effect of the magnetic local time dependence on the conductance, two local time sectors, say 12-19 MLT and 19-22 MLT are chosen as examples and the relationships in the sectors are shown in the left and right panels of the same figure, respectively. The best fit curves are drawn by employing the form of a power function. No data point is appeared beyond the activity level of about 250 nT in the equatorward half of the eastward electrojet. It is understandable if one takes into account the fact that the College station would be located in the poleward half of it when the auroral electrojet expands equatorward with magnetic activity.

In spite of significant scatter, one can notice that Hall conductance increases gradually with

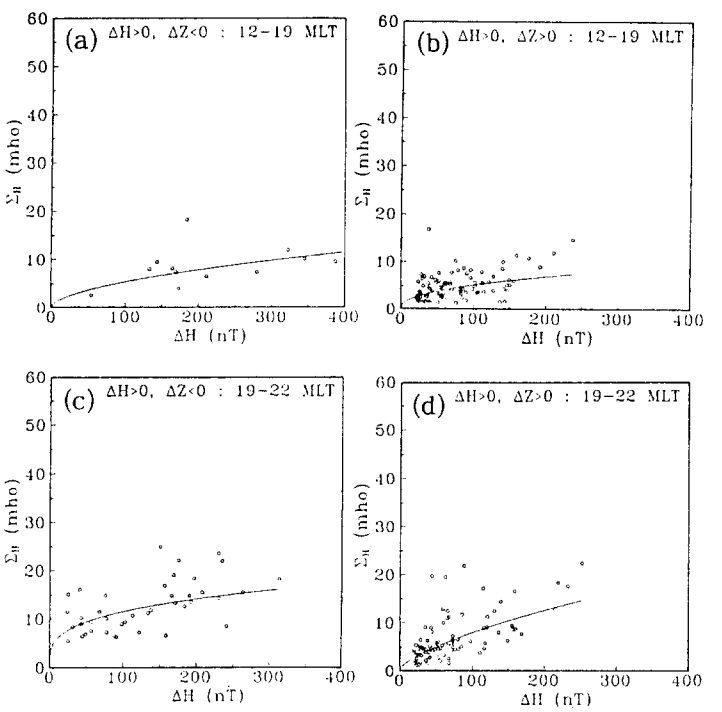

Fig. 1. The relationship between the Hall conductance (Σ_H) measured from the Chatanika incoherent scatter radar and the north-south component (ΔH) of the magnetic disturbance simultaneously observed at College in the four selected regions of the eastward electrojet; the poleward (a) and equatorward (b) halves of it between 12 MLT and 19 MLT, and the poleward (c) and equatorward (d) halves of it between 19 MLT and 22 MLT. The units of conductance and magnetic disturbance are mho and nT, respectively.

magnetic activity for all circumstances. The Hall conductance of the later local time sector (19-22 MLT) shows slightly higher values compared with those of the earlier local time sector (12-19 MLT) for a given level of geomagnetic activity. It is interesting to note that the Hall conductance in Figure 1(c) is no less than 5 mhos in all level of magnetic activity. Although not shown here, the Pedersen conductance shows almost the same tendencies with those of Hall conductance. Furthermore, the Pedersen conductance is quite comparable with the Hall conductance in terms of magnitude during the same level of magnetic activity for all circumstances examined in the eastward electrojet region. It is also worth mentioning that the scatter noted in the relationship between Pedersen conductance and ΔH is less conspicuous than that found between the Hall conductance and ΔH.

The same relationships between the Hall conductance and ΔH in the westward electrojet region are shown in Figure 2 for two selected local time sectors, say 00-02 and 02-04 MLT. One can notice again that there is no data point beyond about 400 nT in the equatorward half of the westward electrojet. It is the same reason mentioned previously. Compared with the eastward electrojet region the Hall conductance in the westward electrojet region is significantly higher, suggesting that the ionospheric conductance enhancement is more important than electric field in the westward electrojet region for a given level of magnetic activity. In particular, it is worth noting that the Hall conductance of the equatorward half of the westward electrojet region is considerably higher than that of the poleward half regardless of the level of magnetic activity. Such a trend is found to be persistent almost over the entire westward electrojet region. Thus the electric field seems to be more important than the ionospheric conductance in the poleward half and vice versa in the equatorward half. On the other hand the Pedersen conductance, not shown here, is generally much smaller than Hall conductance. Neverthless, the general trends

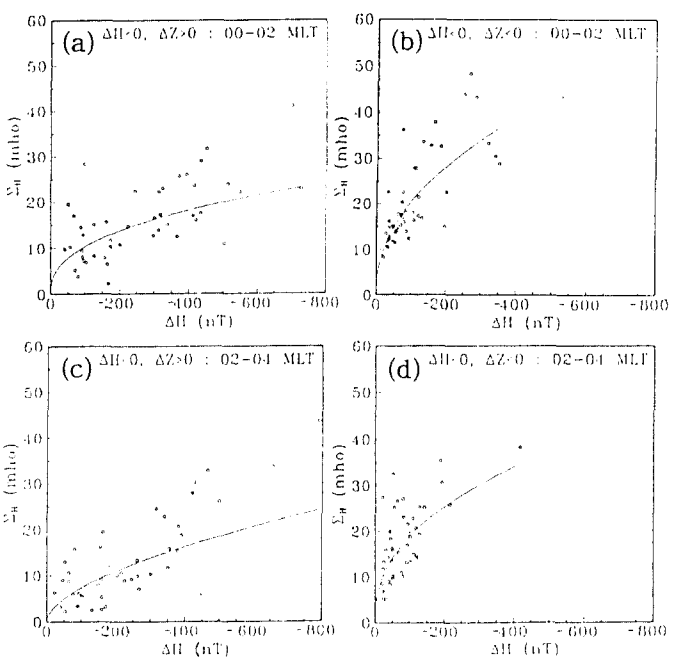

Fig. 2. The same as Figure 1 but for the westward electrojet region in the magnetic local time sectors between 00 MLT and 02 MLT, and between 02 MLT and 04 MLT.

of the dependence of Pedersen conductance upon the MLT and magnetic activity are similar to those of Hall conductance.

To show the dependence of Hall conductance upon magnetic activity and magnetic local time over the entire auroral region, histogram-like diagrams are prepared and are shown in Figure 3. The upper left and right panels show the Hall conductance distributions of the poleward halves of the eastward electrojet and the westward electrojet, respectively. And the lower panels show those of the equatorward halves of the two electrojets. By comparing the conductances estimated during the periods with two different magnetic disturbances levels, say 100 nT and 200 nT in the eastward electrojet region and of -100 nT and -400 nT in the westward electrojet region, it is attempted to show how closely the enhancement of Hall conductance is associated with magnetic activity. The two levels chosen here in each electrojet region are considered to represent the quiet and disturbed periods, respectively. For the estimation of the Hall conductance during a given level of magnetic disturbance in each sector, the empirical formulas obtained from such best fit curves shown in Figures 1 and 2 of the corresponding sector are used.

As shown in Figure 3 one can note that Σ_H during disturbed period (solid curves) is systematically higher than that of quiet period (dotted curves) in all sectors, with the most significant enhancement being noted in the equatorward half of the westward electrojet region. However, the enhancement in the poleward side of the entire auroral electrojet system is not so prominent as that of the equatorward side, thus suggesting that the particle precipitation associated with disturbed period seems to be more concentrated in the equatorward half than the poleward half of the auroral electrojet. It is also worth noting that the conductance enhancement for a given level of magnetic activity seems to be closely associated with magnetic local time. In particular, the enhancement of the midnight sectors between 22 and 24 MLT in the eastward electrojet region and between 22 and 02 MLT in the westward electrojet region during disturbed period are most significant.

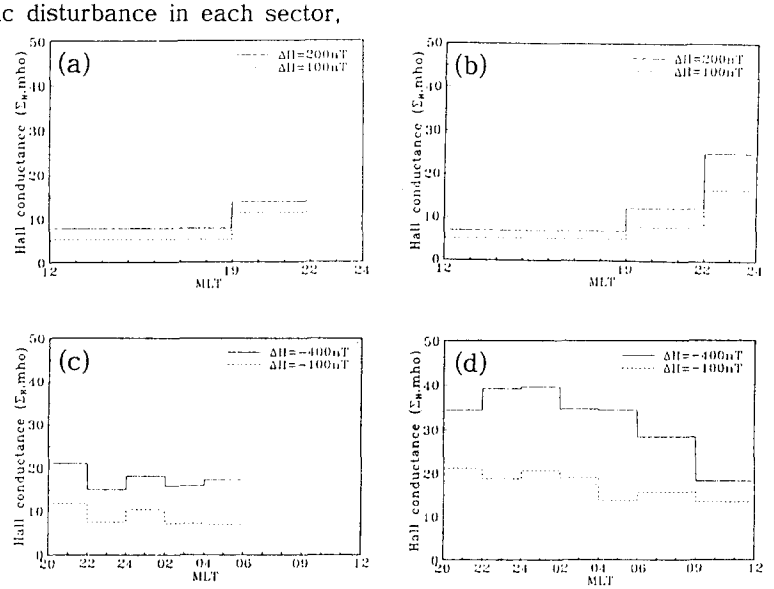

Fig. 3. The Hall conductance distribution as a function of MLT for the four sectors of the auroral electrojets; the poleward (a) and equatorward (b) halves of the eastward electrojet, and the poleward (c) and equatorward (d) halves of the westward electrojet. The solid and dotted lines represent the Hall conductance distributions during the two selected levels of magnetic activity; 100 nT and 200 nT for the eastward electrojet region and -100 nT and -400 nT for the westward electrojet region.

(2) Energy spectrum of precipitating electrons

To estimate the energy spectrum of precipitating electrons the conductance ratios (Σ_H/Σ_P) are examined. Figures 4a and 4b show the relationships between Σ_H and Σ_P in the poleward and equatorward halves of the eastward electrojet in the 19-22 MLT sector, respectively. One can notice that there are significant correlations between the two quantities particularly in the equatorward half (b), suggesting that the average energy of the electrons precipitating into the region is fairly constant and is about 3 keV according to Eq. (2). Figures 4(c) and 4(d) show how the ratio changes with magnetic activity in the poleward and equatorward halves, respectively. One can note that the particle energy expressed in terms of the conductance ratio is more or less constant regardless of magnetic activity. It is particularly the case in the poleward half of the eastward electrojet (c) with the ratio being about 1, while the average energy of the electrons precipitating into the equatorward half shows a moderate increase with magnetic activity.

The conductance ratio in the westward electrojet region is also examined. Figures 5a and 5b show the ratios in the poleward and equatorward halves between 00 MLT and 02 MLT, respectively. As in the eastward electrojet region, one can note that there are significant correlations between the two quantities, with the ratios being 1.58 and 2.01 in the poleward and equatorward halves, respectively. The average energy based on them are thus found to be 4.38 keV and 5.82 keV, respectively, indicating that the particles precipitating into the equatorward half are more energetic than those into the poleward half. Furthermore, it suggests that the average energy of precipitating electrons in the entire westward electrojet region are considerably higher than those in the eastward electrojet region. It is also interesting to note that the conductance ratios in the westward electrojet region are closely associated with magnetic activity with the trend being more significant in the equatorward half. The significant departure of data points from the regression line beyond

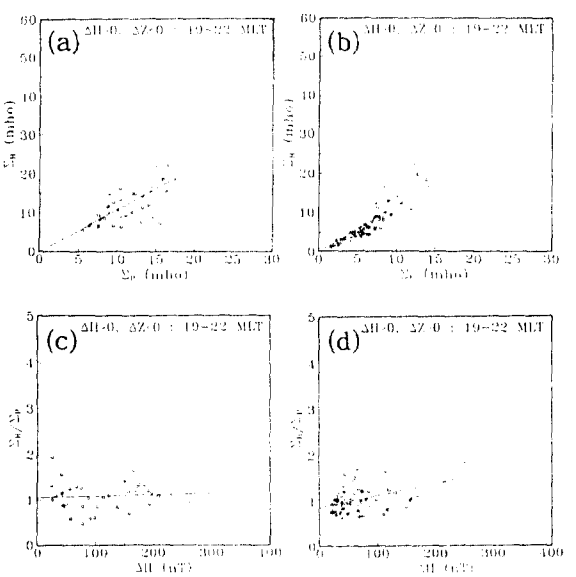

Fig. 4. The relationship between Hall (Σ_H) and Pedersen Conductance (Σ_P) in the eastward electrojet between 19 MLT and 22 MLT is shown in the upper panel. Also shown in the lower panel is the relationship between conductance ratio (Σ_H / Σ_P) and the north-south component (ΔH) of the magnetic disturbance. The left and right panels correspond to the relationships in the poleward and equatorward halves of the eastward electrojet, respectively.

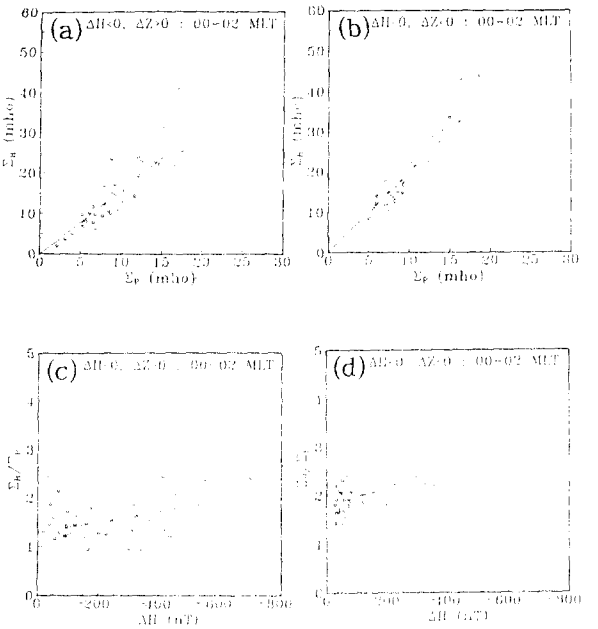

Fig. 5. The same as Figure 4 but for the westward electrojet region between 00 MLT and 02 MLT.

Σ > 15 mhos in Figure 5(b) seems to reflect such a trend. Thus the hardening of particle energy in the westward electrojet region is more closely subject to magnetic activity than that in the eastward electrojet region.

The average energies of the precipitating electrons seem to be closely associated with magnetic local time sector as shown in Figure 6. They are generally harder in the westward electrojet region (b) than in the eastward electrojet (a). More specifically the spectrum gets harder as one goes from the afternoon sector to the late morning sector. The minmum energy of about 2.5 keV and the maximum of about 9.0 keV are registered in the afternoon sector and in the morning sector around 06-09 MLT, respectively. Since the particle energy does not seem to be very sensitive to the magnetic activity except in the equatorward half of the westward electrojet region, it is not attempted to estimate the average energy at different magnetic activity level. However, their spatial variation with respect to the center of auroral electrojet are examined and shown in Figure 6 with the solid and dotted lines being the average energies in the equatorward and poleward halves of auroral electrojets, respectively.

It is interesting to note that the average energy of the electrons precipitating into the westward electrojet region in the prenoon sector (09-12 MLT) is significant higher than that of the electrons into the eastward electrojet region in the postnoon sector (12-19 MLT). It seems that the noon meridian marks a boundary between hard and soft electrons. However, no significant difference is noted in the midnight sector, where the two kinds of auroral electrojets are frequently colocated. On the other hand the average energy of precipitating electron does not show any close association with the latitudinal position with respect to the center of the electrojets. Actually one can notice from Figure 6 that the differences between the solid and dotted lines which represent repectively the average energies of electrons precipitating into poleward and equatorward halves of both auroral electrojet regions are negligible.

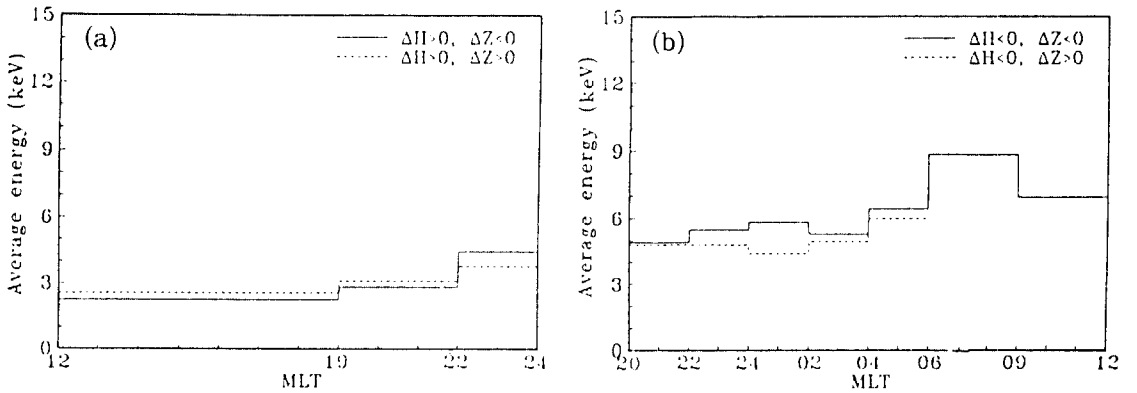

Fig. 6. The average energy of precipitating electrons is shown as a function of magnetic local time; the eastward electrojet region (a) in the left panel and the westward electrojet region (b) in the right panel. The solid and dotted lines represent the energies in the poleward and equatorward halves of the auroral electrojets, respectively. The unit of energy is keV.

(c) The energy flux of precipitating electrons

Since energy flux and the average energy of precipitating electrons are known to be closely associated with ionospheric conductances [*Robinson et al.*, 1987], we are also able to estimate the energy flux based solely on ground magnetic disturbance as the same way we did in estimating the average energy of precipitating electrons. Figure 7 shows the energy flux thus estimated for two magnetic activity levels, say, 100 nT and 200 nT for the eastward electrojet region and -100 nT and -400 nT for the westward electrojet region. The energy fluxes in the poleward and equatorward halves of the eastward electrojet region are shown in Figures 7(a) and 7(b), respectively. And Figures 7(c) and 7(d) denote those in the poleward and equatorward halves of the westward electrojet region, respectively.

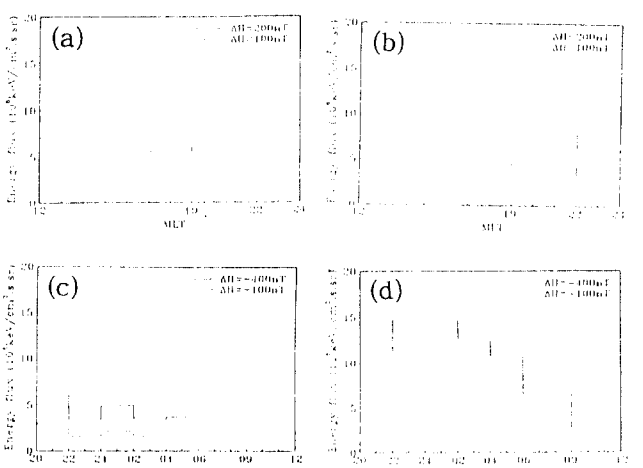

Fig. 7. The same as Figure 3 but for the energy fluxes of precipitating electrons into the auroral region. The unit of the flux is 10^8 keV/cm^2 · sec · sr

Contrary to the average energy of precipitating electrons, the energy flux seems to be more closely associated with magnetic activity. It is particularly the case in the equatorward half of the westward electrojet, where the maximum energy flux is registered about 5 X 10^8 keV/cm^2 · s · sr in the midnight sector during the period with magnetic activity level of -100 nT. But it increased as much as by a factor of three when the magnetic disturbance reached -400 nT. The overall energy flux of the entire sunlit hemisphere spanning from 4 MLT to 19 MLT during quiet period is generally insignificant with only appreciable flux being noted in the poleward half of the eastward electrojet region. Since it is larger than that of the equatorward half by a factor of three, there seems to be some background precipitation in the poleward half even during quiet period. Such precipitations with a comparable energy flux are also noted in the night hemisphere. Note the sectors between 19 MLT and 22 MLT of the equatorward half and from 22 MLT to the midnight of the poleward half of the eastward electrojet and the sector between 20 MLT and 04 MLT of the equatorward half of the westward electrojet. It is also worth mentioning that the energy flux in the poleward half of the westward electrojet region is considerably low compared with that of the equatorward half. As the magnetic activity increases, the energy flux of the entire auroral region also increases. In particular, the enhancements of the equatorward half of the westward electrojet region is remarkable.

It is interesting to point out that the gross patterns of Hall conductance in Figure 3 are very similar to those of energy flux in Figure 7, indicating that the enhancement of Hall conductance with magnetic activity is primarily controlled by the intensification of particle fluxes over the entire auroral electrojet region. However, the equatorward half of the westward electrojet region in the prenoon sector (09-12 MLT) seems to be an exception, where a considerably high Hall conductance, about 20 mhos, is registered regardless of the degree of magnetic activity while the energy flux of the region is insignificant as shown in Figure 7(d). Thus it is quite likely that the average energy of precipitating electrons over the region should be fairly high to explain the large Hall conductance. This is the case what Figure 6(b) shows. In other word the high Hall conductance in the prenoon sector of the equatorward half of the westward electrojet region is closely associated with the hardening of the energy spectrum of precipitation electrons.

3. Summary and Discussions

The ionospheric conductance measurements from the Chatanika incoherent scatter radar and magnetic disturbance data simultaneously obtained from the nearby College magnetic station are compared. The empirical formulas between the two quantities thus obtained enable us to estimate ionospheric conductance distribution from ground magnetic disturbance data. They further make it possible to infer the characteristics of electrons precipitating into the auroral region. Several interesting features noted in this study are :

(1) The Hall conductance in the westward electrojet region is significantly higher than that in the eastward electrojet region for a given level of magnetic activity. More specifically the Hall conductance in the equatorward half of the westward electrojet is much higher than that in the poleward half. However, no such characteristics are noted in the eastward electrojet. The maximum Hall conductance is registered in the equatorward half of the westward electrojet region in the midnight sector between 22 MLT and 02 MLT.

(2) The average energy of precipitating electrons does not seem to be very sensitive to magnetic activity. Particularly, it is the case in the eastward electrojet region. Furthermore,

the energy spectrum does not show any clear spatial variation with respect to the center of auroral electrojets. On the other hand the average energy of electrons gets harder from the postnoon sector to morning setor through the midnight sector with the maximum value, ~ 9 keV, being recorded between 06 and 09 MLT.

(3) The energy flux of precipitating electrons show very similar spatial characteristics with those of Hall conductance, thus indicating that the conductance enhancement is more closely associated with the flux increase than with the hardening of the electron spectrum. The most prominent energy flux during disturbed period is registered in the equatorward half of the westward electrojet between 20 MLT and 09 MLT. Even during quiet period the precipitations in the poleward half of the eastward electrojet region and the equatorward half of the westward electrojet sector between 20 MLT and 04 MLT are considerable.

It is interesting to compare the present result with the satellite measurements by *Hardy et al.* [1985]. The statistical study shows that the average energy of the precipitating electrons has significant magnetic local time variation with the highest being on the morningside oval between 06 MLT and 12 MLT. This is consistent with the present study. Furthermore, they pointed out that the average energy of electrons increases approximately by a factor of 2 between kp = 0 and 3 and is constant for higher kp while the energy flux increases by a factor of more than ten. Almost comparable intensifications in the average energy and energy flux have also been noted in the present study.

It is appropriate to quote several values from their study for a further quantitative comparison with the present ones. The average energy and energy flux during the moderately disturbed period (Kp = 3) are 3.9 keV and 7 X 10^8 keV/cm^2 · sec · sr in the postmidnight sector (~02 MLT) and 6.40 keV and 1.38 X 10^8 keV/cm^2 · sec · sr in the prenoon sector (~10 MLT), respectively. Before being compared with theirs, the present results estimated in the poleward and equatorward halves of the electrojet should be averaged, since their results are considered to be the mean value of the two halves. The four values thus estimated are 5 keV, 8 X 10^8 keV/cm^2 · sec · sr, 7 keV and 2.7 X 10^8 keV/cm^2 · sec · sr. One can notice that the two results are remarkably comparable. Therefore, it may be possible to assess the characteristics of electrons precipitating into the auroral region by the simple empirical formulas derived in this study using ground mangetic disturbance data as input. Furthermore, this method has an advantage over the statistical method in that it is possible to provide a global 'instantaneous' distribution patterns of precipitating electrons as far as the corresponding ground magnetic distrubance data employed for this purpose are instantaneous. The patterns thus prepared in this study can also show the latitudinal variations of these quantities while they are lost in satellite measurements due to its averaging process.

Acknowledgement

This work was partially supported by the Korea Research Foundation, 1994. B.-H. A. acknowledges the generous hospitality of the NOAA's National Geophysical Data Center and the High Altitude Observatory of the National Center for Atmospheric Research during his short visit in the summer of 1993. We would like to thank Drs. Art Richmond and Herb Kroehl for their useful discussions on the subject dealt in this paper. The ionospheric conductance data has been kindly provided by Dr. Odile de Beaujardiere with SRI International, now at National Science Fournation.

References

Ahn, B.-H., R.M. Robinson, Y. Kamide, and S.-I. Akasofu, Electric conductivities, electric fields and auroral particle energy injection rate in the auroral ionosphere and their empirical relations to the horizontal magnetic disturbances, *Planet. Space Sci.*, *31*, 641, 1983.

Foster, J.C., Reply to Kamide and Richmond, *Geophys. Res. Lett.*, *14*, 160, 1987.

Fuller-Rowell, T.J., and D.S. Evans, Height-integrated Pedersen and Hall conductivity patterns inferred from the TIROS-NOAA satellite data, *J. Geophys. Res.*, *92*, 7606, 1987.

Hardy, D.A., M.S. Gussenhoven, and E. Holeman, A statistical model of auroral electron precipitation, *J. Geophys. Res.*, *90*, 4229, 1985.

Hardy, D.A., M.S. Gussenhoven, R. Raistrick, and W.J. McNeil, Statistical and functional representations of the pattern of auroral energy flux, number flux and conductivity, *J. Geophys. Res.*, *92*, 12275, 1987.

Kamide, Y., *Electrodynamic Processes in the Earth's Ionosphere and Magnetosphere*, Kyoto Sangyo University Press, Kyoto, Japan, 1988.

Kamide, Y., A.D. Richmond, and S. Matsushita, Estimation of ionospheric electric field, ionospheric currents, and field-aligned currents from ground magnetic records, *J. Geophys. Res.*, *86*, 801, 1981.

Lummerzheim, D., M.H. Rees, J.D. Craven, and L.A. Frank, Ionospheric conductances derived from DE-1 auroral images, *J. Atmos. Terr. Phys.*, *53*, 281, 1991.

Rees, M.H., Auroral energy deposition rate, *Planet. Space Sci.*, *40*, 299, 1992.

Rees, M.H., D. Lummerzheim, R.G. Roble, J.D. Winningham, J.D. Craven, and L.A. Frank, Auroral energy deposition rate, characteristic electron energy and ionospheric parameters derived from Dynamic Explorer 1 image, *J. Geophys. Res.*, *93*, 12841, 1988.

Richmond, A.D., and Y. Kamide, Mapping electrodynamic features of the high-latitude ionosphere from localized observations : Technique, *J. Geophys. Res.*, *94*, 5741, 1988.

Robinson, R.M., F. Rich, and R.R. Vondrak, Chatanika radar and S3-2 measurements of auroral zone electrodynamics in the midnight sector, *J. Geophys. Res.*, *90*, 8487, 1985.

Robinson, R.M., and R.R. Vondrak, Measurements of E region ionization and conductivity produced by solar illumination at high latitudes, *J. Geophys. Res.*, *89*, 3951, 1984.

Robinson, R.M., R.R. Vondrak, K. Miller, T. Dabbs, and D. Hardy, On calculating ionospheric conductances from the flux and energy of precipitating electrons, *J. Geophys. Res.*, *92*, 2565, 1987.

Spiro, R.W., P.H. Reiff, and L.J. Mather, Jr., Precipitating electron energy flux and auroral zone conductivities - An empirical model, *J. Geophys. Res.*, *87*, 8215, 1982.

Wallis, D.D., C.D. Anger, and G. Rostoker, The spatial relationship of auroral electrojets and visible aurora in the evening sector, *J. Geophys. Res.*, *81*, 2857, 1976.

Wallis, D.D., and E.E. Budzinski, Empirical models of height integrated conductivities, *J. Geophys. Res.*, *86*, 125, 1981.